

## Surface sediment effects on teleseismic *P* wave amplitude

Ying Zhou, Guust Nolet, and F. A. Dahlen

Department of Geosciences, Princeton University, Princeton, New Jersey, USA

Received 3 December 2002; revised 25 April 2003; accepted 7 May 2003; published 9 September 2003.

[1] Teleseismic *P* waves are dominated by relatively low frequency (<1 Hz) signals due to the Earth's attenuation; because of this, receiver site effects are usually assumed to be independent of frequency. We investigate the site amplitude effects due to a surface sediment layer and show that teleseismic frequency-dependent site effects can be important. One-dimensional modeling shows that the effects of amplification due to differences in impedance, combined with amplitude losses to reverberations in the sediment layer, can result in significantly frequency-dependent site effects. The extent of the frequency dependence depends upon the two-way travel time of *P* waves in the sediments and the dominant period of the *P* waves. Using model CRUST2.0, we compute a  $2^\circ \times 2^\circ$  map of the "reference" period of *P* waves above which the dependency can be neglected. We argue that the common practice of applying station corrections to magnitude determination will underestimate the magnitude of large earthquakes. To show that these effects are observable in practice, we analyze the amplitude ratios of seven teleseismic events at the station pair KURK and MAKZ and six events at the station pair KMI and CHTO. The amplitude ratios are relatively insensitive to other contributing effects and are in good agreement with the predicted frequency-dependent effects of the surface sediment layer. *INDEX TERMS*: 7203 Seismology: Body wave propagation; 7205 Seismology: Continental crust (1242); 7212 Seismology: Earthquake ground motions and engineering; 7260 Seismology: Theory and modeling; *KEYWORDS*: *P* wave amplitude, sediment, magnitude, receiver functions

**Citation:** Zhou, Y., G. Nolet, and F. A. Dahlen, Surface sediment effects on teleseismic *P* wave amplitude, *J. Geophys. Res.*, 108(B9), 2417, doi:10.1029/2002JB002331, 2003.

### 1. Introduction

[2] Teleseismic *P* wave amplitudes are exploited in body wave magnitude determinations [Nuttli, 1972]. Occasionally, they have also been used to provide constraints on the Earth's elastic and anelastic structure [Anderson and Hart, 1978; Haddon and Husebye, 1978; Neele et al., 1993]. However, amplitudes are affected by many processes, including the source radiation pattern, attenuation, scattering, focusing/defocusing and receiver or site effects. It is always a difficult problem to isolate those effects to study the processes separately. The significance of the site effects on seismic amplitudes has been studied for a long time, but to date those studies have mainly concentrated on the *S* wave spectra of local and regional earthquakes [King and Tucker, 1984; Vernon et al., 1998; Al-Shukri et al., 1995]. The elastic properties in the first few kilometers (e.g., sediment, weathering layers) are known to be responsible for strong frequency-dependent site effects. However, little attention has been paid to teleseismic *P* wave amplitude anomalies, although *P* wave amplitudes have been observed to vary considerably over short distance [Berteussen, 1975]. The frequency-dependent nature of the site effects on the *P*

wave amplitudes has also been noticed indirectly in body wave magnitude determination: Husebye et al. [1974] proposed that the station correction for earthquake magnitude may be a function of magnitude.

[3] Observed amplitudes used in magnitude determinations are commonly corrected for the site effects by applying station corrections that are frequency-independent. It is important to fully understand the significance of the site effects and, importantly, whether their dependence on frequency is truly negligible. The frequency dependence of teleseismic *P* wave amplitudes is the topic of this paper. Other local effects such as Moho topography and near-receiver scattering have been shown to be small in the frequency band considered in this paper [Nolet and Dahlen, 2000].

### 2. Simple Sediment Layer Model

[4] Ground displacements recorded by seismometers are influenced by the free-surface boundary, which generates reflected and converted waves. In the presence of a sedimentary layer, the *P* wave displacements are amplified as they travel from high-impedance media into the surface low-impedance media to conserve energy. In addition to the low-impedance amplification, the *P* wave amplitude may also be affected by energy loss at the bottom and by strong reverberations in the sediment layer. Only if the two-way

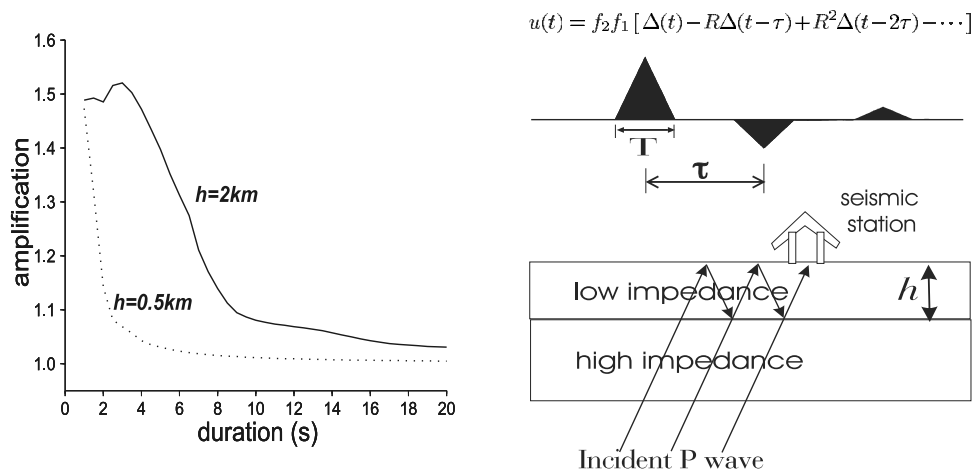


**Figure 1.** (left) Frequency-dependent  $P$  wave amplification by a sediment layer, calculated for a triangle pulse shape  $P$  wave at epicentral distance of  $\sim 60^\circ$ . The amplification curves are computed using a two-layer model in Figure 1 (right). The thickness of the top sediment layer is  $h = 2$  km (solid line) and  $h = 0.5$  km (dotted line), respectively. (right) Cartoon illustrating the amplification effects of the low impedance and the “deamplification” effects of the reverberations.  $T$  is  $P$  wave duration;  $\tau$  is two-way  $P$  wave travel time in the sediment,  $f_1$  is the transmission coefficient across the low/high impedance interface,  $R$  is the total reflection coefficient for one peg-leg, and  $f_2$  is the free-surface effect.

travel time in the sediment layer is very small with respect to the wave period do these reverberations interfere destructively with the first arrival (in the limit of a very thin layer they can be shown to add up to the original amplitude in the bedrock). We perform our calculations for a fully elastic model; however, the effects of  $P$ -to- $S$  conversions are very small on the vertical component due to the steep incident angles of the teleseismic waves in the sediment layer.

[5] We use a simple two-layer model (Figure 1) to illustrate the site amplification effects due to a surface sediment layer beneath the station. The  $P$  wave velocity is 2.0 km/s in the sediment and 4.5 km/s in the underlying bedrock. We assume that the  $P$  wave displacement has a triangle pulse shape, and we define the root-mean-square amplitude,  $A$ , by

$$A = \sqrt{\frac{1}{T} \int_0^T u^2(t) dt}, \quad (1)$$

where  $u(t)$  is the seismogram of the vertical displacement, calculated using a matrix propagator method for elastic waves. The averaging length  $T$  is the first zero-to-zero duration in the  $P$  wave seismogram. In the presence of significant noise, the definition (1) of  $A$  is more stable than the usual peak-to-peak amplitude measurement [Tibuleac *et al.*, 2003]. Both the peak-to-peak measurement and equation (1) have in common that they are influenced by sedimentary reverberations in a nonlinear way.

[6] The amplification in Figure 1 is defined as the amplitude normalized with respect to the amplitude in the half-space. Figure 1 shows the sediment amplification as a function of  $P$  wave pulse duration  $T$  at an epicentral distance of  $\sim 60^\circ$  (horizontal slowness  $p = 7$  s/deg). Clearly, the relation between the site amplification and the pulse duration of the  $P$  wave exhibits three regimes: (1) the amplification reaches its maximum when the pulse duration of the incident  $P$  wave is shorter than the two-way  $P$  wave travel time  $\tau$  in

the sediment layer; (2) as the pulse duration of the incident  $P$  wave becomes longer than the two-way travel time  $\tau$ , the amplification is reduced by the  $P$  wave reverberations; and (3) finally, the reverberations can cancel out the amplification effects completely when the pulse duration  $T$  is much longer than  $\tau$ , so that the total amplification approaches unity. As the thickness of the sediment layer decreases, the range in which amplifications are significantly frequency-dependent is limited to shorter periods.

[7] These computations were done for constant sediment velocity. To investigate the effects of consolidation of sediments, we use a stair-step model with the compaction simulated by a typical velocity-depth relation  $v = v_0 z^k$ , where  $k = 1/6$  [Faust, 1951] and  $v_0 = 2.5$  km/s, and compare the amplification curve with that of a uniform sediment layer model (Figure 2). The comparison confirms that it is acceptable to neglect the sediment compaction effects in the frequency range of our study.

[8] Because the sedimentary layer is thin and the frequencies of interest are below 1 Hz, we neglect any effects of attenuation in the sediment layer. Since large earthquakes usually radiate  $P$  waves of longer period, our modeling implies that frequency-independent station corrections tend to overcorrect the amplitudes of large events and under correct those of small events, whenever sediment underlies seismic stations. The commonly used station corrections are obtained by averaging the  $P$  wave amplitudes of different earthquakes, assuming the path effects are averaged out. Since small earthquakes dominate in the average, this procedure leads to underestimation of the magnitude of larger earthquakes.

### 3. Surface Sediments Beneath the Seismic Stations: Global Statistics

[9] In this paper, we use a global crustal model CRUST2.0 (G. Laske *et al.*, CRUST2.0—A new global crustal model at

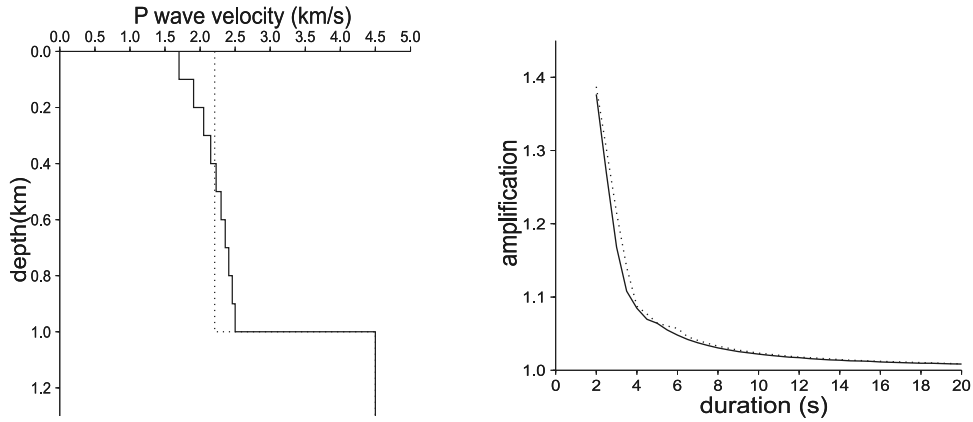


**Figure 2.** (left) The dotted line is a one-layer sediment model; solid line represents the unconsolidated sediment model, which consists of 10 sublayers with a velocity-depth ( $v-z$ ) relation  $v = v_0 z^k$ ,  $k = 1/6$ , and  $v_0 = 2.5$  km/s. The mean  $P$  wave velocities in the sediments are 2.2 km/s in both models. (right) The dotted line is the corresponding frequency-dependent amplification curve of the one-layer sediment model; the solid line is the frequency-dependent amplification curve of the unconsolidated sediment.

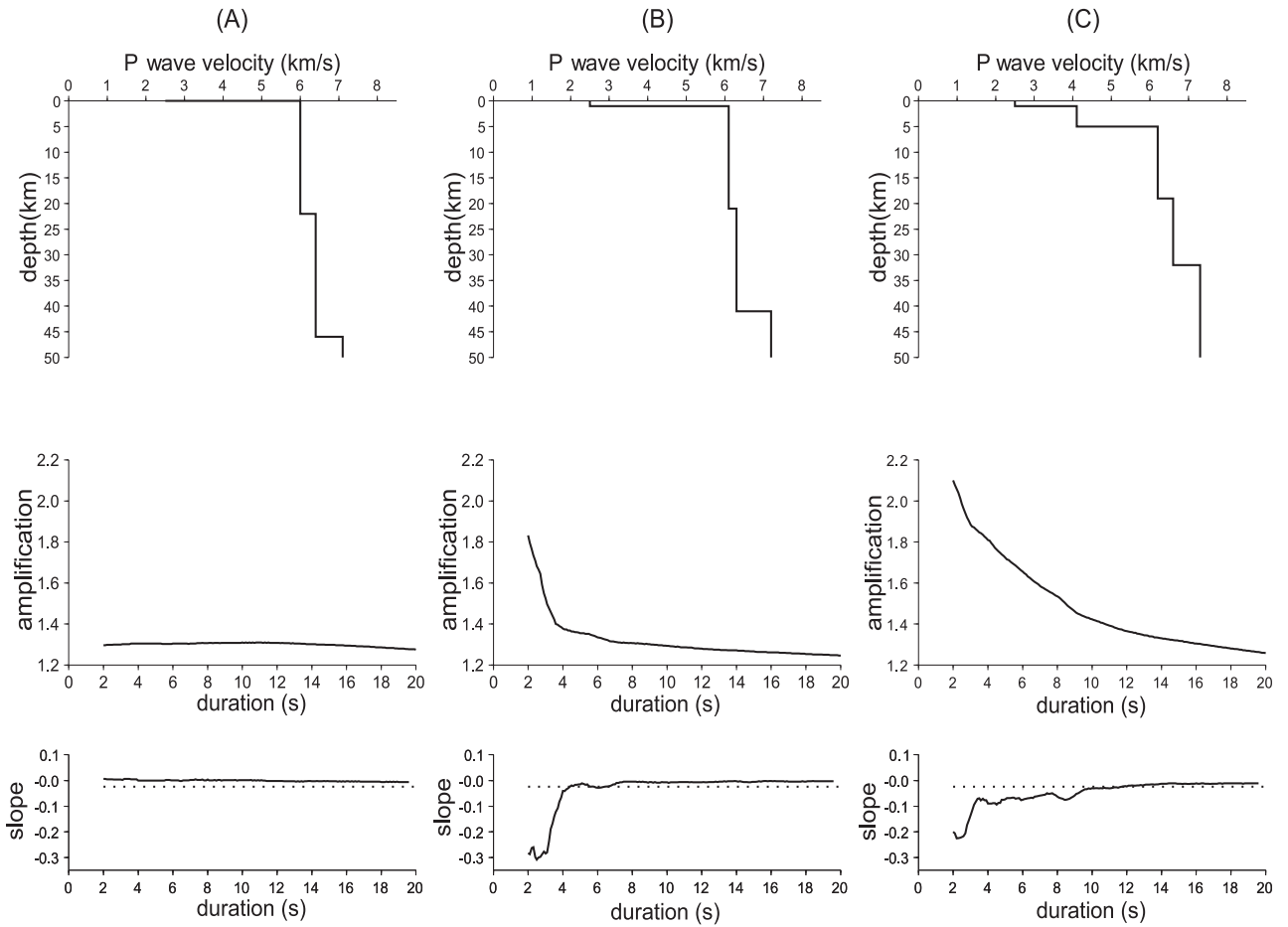


**Figure 3.** (top) Three representative crustal models selected from CRUST2.0 at the site of three GSN seismic stations (a) LSA, (b) AAK, and (c) YAK. (middle) The corresponding frequency-dependent amplification curves. The amplifications are with respect to the amplitude without the crustal effects. (bottom) the slope of the amplification curves as a function of  $P$  wave pulse duration. The dotted line has a constant slope value of  $dA/dT = -0.025$ .

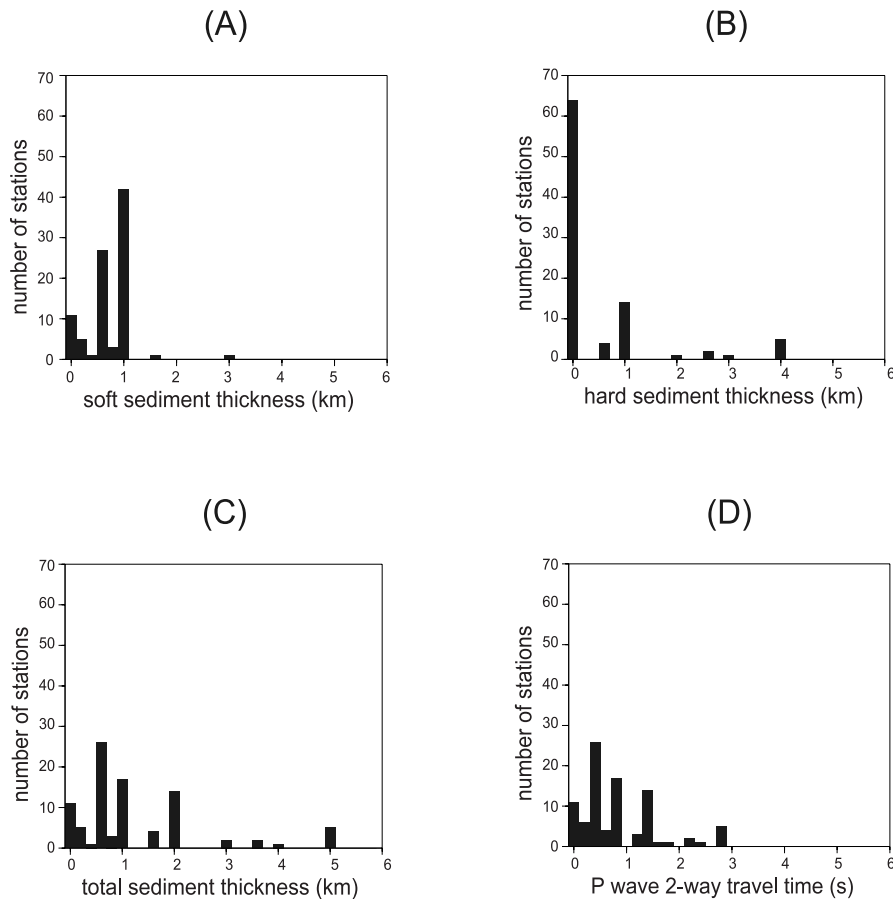


**Figure 4.** Statistics on the sediment thickness at 91 GSN stations, assuming the  $2^\circ \times 2^\circ$  global crust model CRUST2.0 is adequate. (a) Soft sediment thickness; (b) hard sediment thickness; (c) total sediment thickness; (d)  $P$  wave vertical two-way travel time in the sediment.

$2 \times 2$  degrees, 2001, available at <http://mahi.ucsd.edu/Gabi/crust2.html>). to estimate the importance of potential site effects for typical seismic stations. CRUST2.0 is a seven-layer crustal model in each  $2^\circ \times 2^\circ$  global cell, which specifies the  $P$  wave and  $S$  wave velocities as well as the densities in each crustal layer and in the mantle lid. Three models are selected in this paper to represent the typical crustal structure beneath the seismic stations (Figure 3). Model A has no sediment layer, the amplification curve is independent of frequency, and the constant degree of amplification ( $\sim 1.3$ ) is due to the lower impedance in the crust than that in the mantle lid. Model B has 1 km of soft sediment ( $V_p = 2.5$  km/s), the corresponding amplifications are significantly frequency dependent, and the significance becomes negligible for  $P$  waves with relatively long pulse duration. Model C has 1 km of soft sediment and 4 km of hard sediment ( $V_p = 4.0$  km/s), and the amplifications are more significantly frequency-dependent compared to model B. The slope of the amplification curve  $dA(T)/dT$ , where  $A(T)$  is the amplification of a  $T$ -second  $P$  wave, is a quantified measure of the significance of the frequency dependency. Notice that amplification consistently decreases with increasing pulse duration. We use a slope of  $dA/dT = -0.025$  as a threshold, above which the amplification can be regarded as frequency-independent. We use a list of 91 GSN station locations as representative for the statistical distribution of seismic stations over the crustal structures repre-

sented in CRUST2.0. Figure 4 shows that sediments underly most stations, but the thickness usually does not exceed 2 km, and the vertical two-way  $P$  wave travel time  $\tau$  in the sediments is generally less than 3 s. These statistics show that model B in Figure 3 is representative for the sediment structure beneath many stations. We may presuppose that stations are located on bedrock with a velocity higher than 2.5 km/s of the top layer in model B. Still, we consider model B (Figure 3) representative because (1) the thin top layer has a minor effects (Figure 1), and (2) the teleseismic  $P$  waves and their reverberations sample a wide range around the station.

[10] Model CRUST2.0 provides an opportunity to estimate the crustal site effects on a global scale. We calculate the site amplification in each of the  $2^\circ \times 2^\circ$  global cells, for incident  $P$  waves with a horizontal slowness of 7 s/deg, or equivalently, an epicentral distance of  $\sim 60^\circ$ . The continental map of the “reference” pulse duration is plotted in Figure 5. If the  $P$  wave period of interest exceeds this “reference” period, the sediment effects on the teleseismic  $P$  waves can be considered as independent of frequency. Notice that the ice layer is treated as a sediment layer as far as its seismic velocity is concerned. The regions associated with a long reference period (red) coincide with regions with thick surface sediments.

[11] In general, the site effects are dominated by the surface sediment layer because of the large impedance

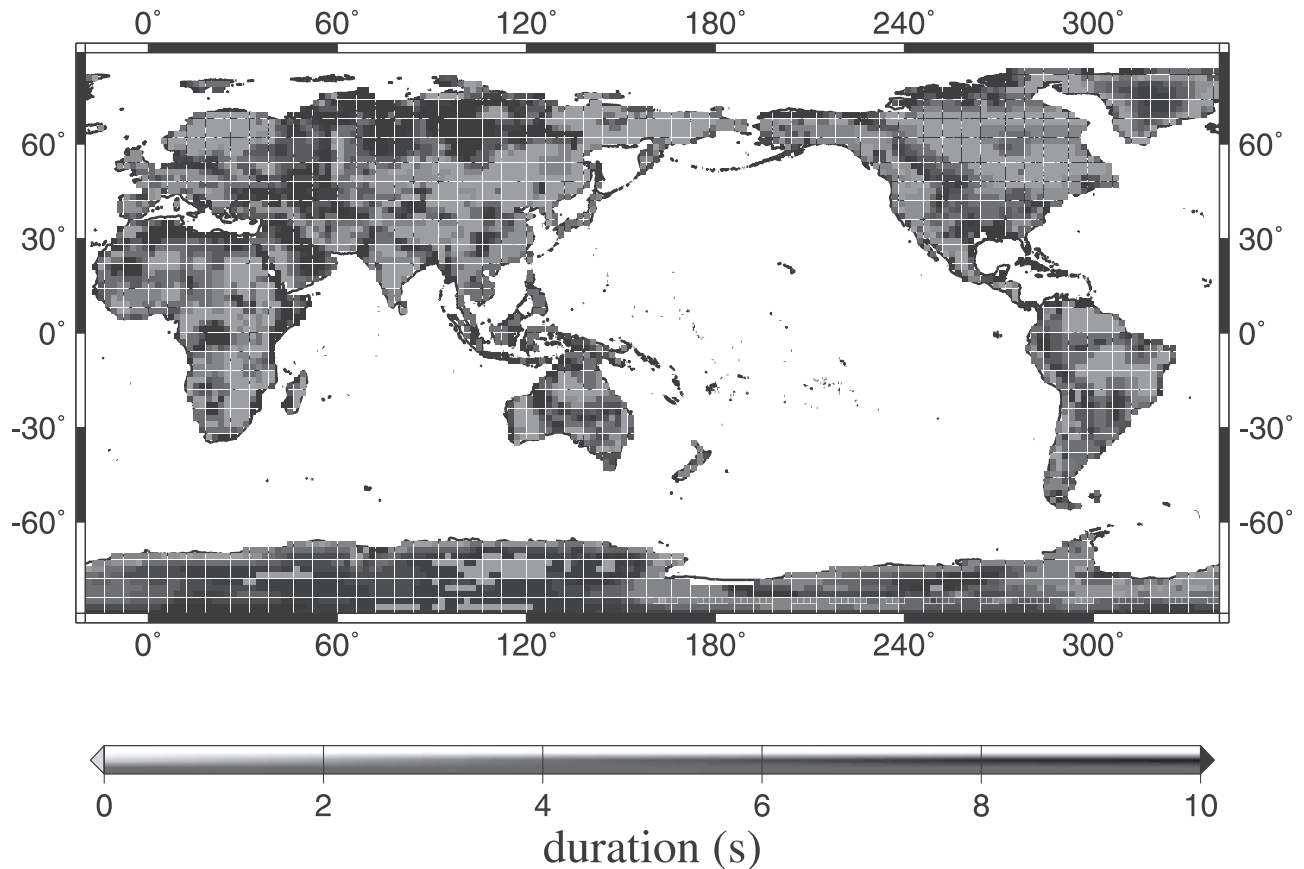


**Figure 5.** Map of the “reference” period above which the crustal amplification of teleseismic  $P$  wave can be regarded as frequency independent (the amplification slope  $dA/dT > -0.025$ ). See color version of this figure at back of this issue.

contrast at the sediment/bedrock interface. There are also small contributions from the layered structure of the whole crust; for example, the upper crust affects the  $P$  wave amplitudes in a similar way to that of a sediment layer due to the small impedance jump at the upper crust/midcrust interface. However, these effects are much smaller than the sediment. Crustal anomalies, such as a low velocity layer in the upper crust, can also introduce frequency-dependent site effects, which can be analyzed in a similar manner as the reverberation effects of the surface sediments.

[12] Near-surface structure may have different effects on a borehole station than on a surface station. However, this difference can be neglected due to the fact that the depth of borehole stations are generally less than 100 m, much smaller than the wavelength of teleseismic waves with dominant frequency well below 1 Hz. For some GSN stations sitting on young sediments, the surface  $P$  wave velocity can be extremely low in the top unconsolidated material, much less than the velocity (1.7 km/s) in the top layer in Figure 2. We assume that this effect is also negligible because the thickness of such an unconsolidated layer is likely to be less than few hundred meters.

#### 4. Measurements of the Amplitude Ratios: Site Effects

[13] A straightforward way to confirm the frequency-dependent amplification effects observationally is to compare

the amplitudes at two nearby seismic stations. For example, if both stations happen to be situated on the hard rock, the amplitude ratios are expected to be nearly independent of the period of the incident  $P$  wave; in contrast, if one station sits on the top of sediments, we expect the amplitude ratio to be dependent upon the dominant  $P$  wave period. In practice, the success of this method depends upon the distribution of the earthquakes as well as upon the data quality. We apply the following selection criteria to study the effects predicted in this study: (1) deep seismic events with epicentral distance between  $45^\circ$  and  $90^\circ$ , such that rays to two nearby stations are closely spaced in the mantle, and the  $P$  waves have steep incidence angle beneath the receiver; (2) event radiations at the receiver azimuth are stronger than 30% of the maximum radiation, assuming the Harvard CMT solution is accurate; this is to limit the effects of the noise and possible bias in the seismic source moment determinations; and (3) the difference between the measured pulse durations at the two stations of a single event is required to be 0.5 s or less.

[14] We use the amplitude data set described by *Tibuleac et al.* [2003]. It is a data set of deep events, originally collected to investigate three-dimensional velocity models of the Earth’s mantle. The amplitudes  $A$  in the data set are measured using the same definition as in this paper (equation (1)). For station pair KURK and MAKZ, seven events meet our selection criteria, and are used in the final analysis. Six events are selected for station pair KMI and



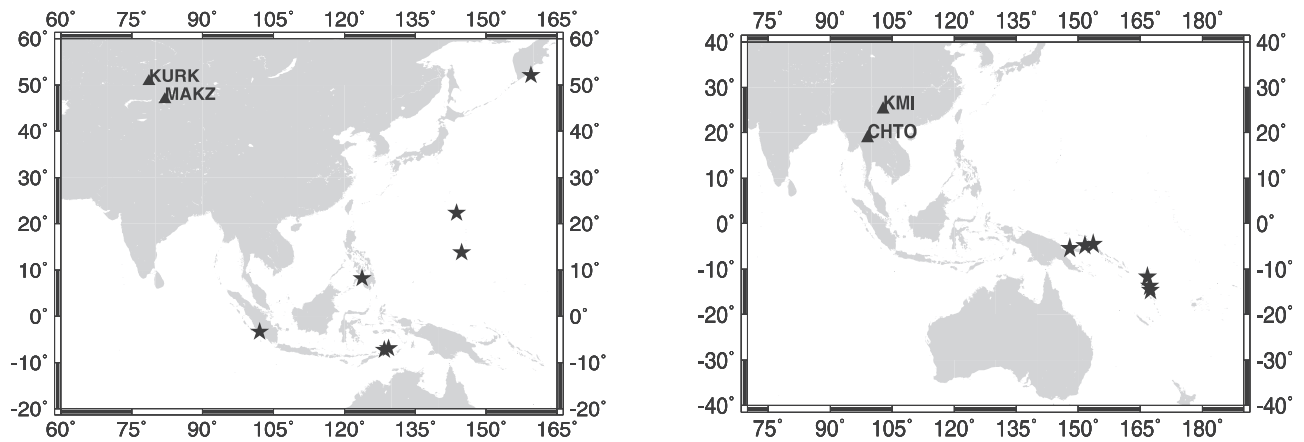


**Figure 6.** (left) Seven deep teleseismic events (stars), recorded at the two neighboring GSN seismic stations, KURK (78.62°E, 50.72°N) and MAKZ (81.98°E, 46.8°N) (Table 1). (right) Six events recorded at station pair KMI (102.74°E, 25.12°N) and CHTO (98.98°E, 18.78°N) (Table 2). The epicentral distances of all events are greater than 45°. The two stations of each station pair differ <5° in the epicentral distance, <10° in the event azimuth, and <0.5 s in the measured pulse duration. All events have strong radiations toward the station direction, within 30% of the maximum radiation.

CHTO. The source and receiver locations are shown in the maps in Figure 6. The event parameters for those events are listed in Tables 1 and 2. The events have a good distribution in the  $P$  wave pulse duration, ranging from 3.8 to 18 s. The measured amplitudes have estimated errors of 10% [Tibuleac *et al.*, 2003], which include errors in source corrections and instrument magnification (Figure 7). For theoretical predictions, we used the site descriptions in the FDSN station book and combined this with known crustal models in nearby provinces. For station KURK, the  $P$  wave velocity in each layer is taken from the fine-layered Kosarev's crustal model of Tien Shan region [Kosarev *et al.*, 1993], averaged over nine layers. For station MAKZ we use the same model, but with the top two sedimentary layers removed following the FDSN station description. Kosarev's Tien Shan model may not be ideal for the Kazakh shield, but it is the only reasonably local crustal information we have available. The crustal structure of station KMI is taken from the crustal model in Yunnan Province, China, proposed by Kan *et al.* [1986] from refraction experiments. The  $P$  wave structure of station CHTO is modified from the crust structure in the southwest China [Chan *et al.*, 2001] by adding a low-velocity layer in the upper crust beneath station CHTO, associated with the high heat flow in the Chiang Mai area, characterized by hot springs confined in faulted and fractured granite [Ramingswong *et al.*, 1978].

[15] The amplitude ratios calculated for the modified local crustal models agree well with the measurements

(Figure 7). In general, it is consistent with the surface sediment effects: short-period  $P$  waves are more amplified at stations with surface sediments. The amplifications show little dependence upon the epicentral distance within the range 45° to 73°. It is noteworthy that the reverberations in the upper crustal low-velocity layer beneath station CHTO deamplifies the short period  $P$  waves, thereby increasing the amplitude ratios of the station pair KMI/CHTO.

## 5. Discussion and Conclusion

[16] The frequency-dependent site effects due to a surface sediment layer can be considerable and should be taken into account if magnitudes or scalar moments are determined from teleseismic  $P$  waves with short dominant periods. The influence of the sediment on the amplitude is the net effect of two competing mechanisms: impedance amplification and deamplification through reverberations. The relative importance of the second effect depends upon the pulse duration  $T$  and on the  $P$  wave two-way travel time  $\tau$  in the sediment. A reduction in the sediment velocity as well as an increase in the sediment thickness leads to a wider range of period over which the site amplifications are significantly frequency-dependent.

[17] A simple statistical analysis based on model CRUST2.0 and the location of 91 GSN stations shows that sediments are likely to underlie most of the stations, and that frequency dependence of amplitudes is important,

**Table 1.** Seven Events Recorded at Stations KURK and MAKZ

Event	Year	Day	Longitude	Latitude	Depth, km	Duration, <sup>a</sup> s
1	1997	112	102.05°	-3.39°	109.0	5.35
2	1998	143	123.73°	8.14°	645.0	4.70
3	1998	147	159.45°	52.08°	48.0	10.69
4	1999	293	129.34°	-6.94°	189.0	3.81
5	2000	57	144.78°	13.80°	132.0	4.40
6	2000	63	128.49°	-7.32°	142.0	3.62
7	2000	88	143.73°	22.34°	127.0	15.48

<sup>a</sup>Average of the measured durations at the two stations.

**Table 2.** Six Events Recorded at Stations KMI and CHTO

Event	Year	Day	Longitude	Latitude	Depth, km	Duration, <sup>a</sup> s
1	1995	226	151.61°	-4.80°	131.0	8.70
2	1996	77	167.46°	-14.66°	160.0	7.00
3	1996	245	166.76°	-11.78°	181.0	5.80
4	1997	356	147.90°	-5.46°	187.0	17.33
5	1999	28	153.66°	-4.58°	101.0	10.32
6	1999	260	167.24°	-13.79°	197.0	5.25

<sup>a</sup>Average of the measured durations at the two stations.

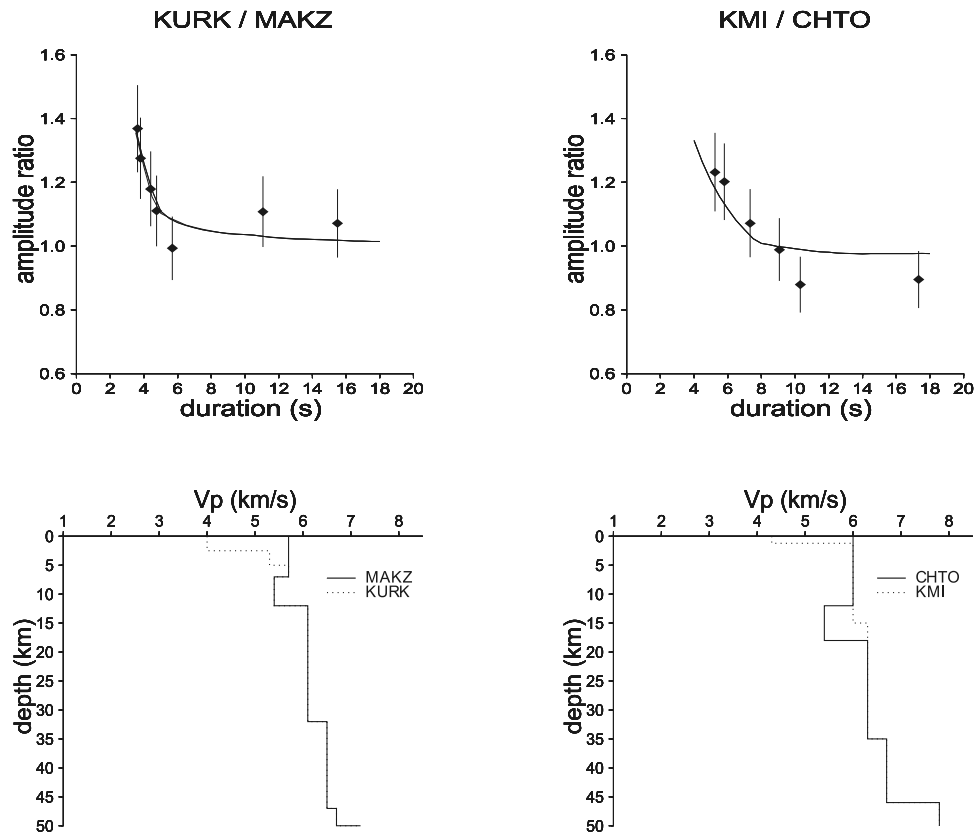


**Figure 7.** (top left) Measured amplitude ratios (diamonds, with error bars) of station KURK and MAKZ for the seven deep events (map in Figure 6). The three solid lines (which overlap mostly) are the calculated amplitude ratios using the  $P$  wave velocity models in the bottom left, for event epicenter distances of  $45^\circ$ ,  $60^\circ$  and  $73^\circ$ , respectively. (top right) the diamonds are the measured amplitude ratios of station KMI and CHTO (map in Figure 6). The solid line is computed using the bottom right velocity models of those two stations for events at epicentral distance of  $60^\circ$ .

certainly for periods below about 5 s. On the basis of empirical relations between the body wave magnitude and the  $P$  wave pulse duration [Kanamori and Anderson, 1975; Bos *et al.*, 1998], we may assume that the frequency-dependent  $P$  wave amplification due to the site effects is most significant for earthquakes with body wave magnitude  $m_b < 5.8$ . To decide whether a frequency-independent station correction is sufficient, one should consider both the thickness of the sediments and the dominant period of the  $P$  wave. To illustrate the importance of the frequency dependence, we analyzed the amplitude ratios of two station pairs, KURK/MAKZ and KMI/CHTO. In general, the ratios behave very much in the way predicted by our simple theoretical model: short-period  $P$  waves are more amplified at the stations overlying a thicker sediment layer. We also discovered that a low impedance layer in the upper crust can introduce frequency-dependent site effects, analogous to the transmission/reverberation effects of the surface sediments. In closing, we note that the reverberations can have similar effects on downgoing as well as upgoing waves. As a result, surface reflected phases such as  $pP$  and  $PP$  can be affected by the sediment layer at the reflection point, thereby introducing frequency-dependent surface effects.

[18] **Acknowledgments.** We thank the Associate Editor Rob van der Hilst and the two reviewers Sébastien Chevrot and Gary Pavlis for their

extensive comments, which greatly contributed to improving the paper. This research was supported by the U.S. NSF under grants EAR-9814570 and EAR-0105387.

## References

- Al-Shukri, H. J., G. L. Pavlis, and F. L. Vernon III, Site effect observations from broadband arrays, *Bull. Seismol. Soc. Am.*, **85**, 1758–1769, 1995.
- Anderson, D. L., and R. S. Hart,  $Q$  of the Earth, *J. Geophys. Res.*, **83**, 5869–5882, 1978.
- Berteussen, K. A.,  $P$  wave amplitude variability at NORSAR, *J. Geophys.*, **41**, 595–613, 1975.
- Bos, A. G., G. Nolet, A. Rubin, H. Houston, and J. E. Vidale, Duration of deep earthquake determined by stacking of Global Seismograph Network seismograms, *J. Geophys. Res.*, **103**, 21,059–21,065, 1998.
- Chan, W. W., C. Y. Wang, and W. D. Mooney, 3-D crustal structure in southwestern China, *Proceedings of the 23rd Seismic Research Review: Worldwide Monitoring of Nuclear Explosions*, edited by L. A. Casey, pp. 12–20, U. S. Dep. of Energy, Natl. Nucl. Security Admin., Washington, D. C., 2001.
- Faust, L. Y., Seismic velocity as a function of depth and geologic time, *Geophysics*, **16**, 192–206, 1951.
- Haddon, R. A. W., and E. S. Husebye, Joint interpretation of P-wave time and amplitude anomalies in terms of lithospheric heterogeneities, *Geophys. J. R. Astron. Soc.*, **55**, 19–43, 1978.
- Husebye, E. S., A. Dahle, and K. A. Berteussen, Bias analysis of Norsar- and ISC-reported seismic events  $m_b$  magnitudes, *J. Geophys. Res.*, **79**, 2967–2978, 1974.
- Kan, R.-J., H.-X. Hu, R.-S. Zeng, W. D. Mooney, and T. V. McEvelly, Crustal structure of Yunnan province, People's Republic of China, from seismic refraction profiles, *Science*, **234**, 433–437, 1986.
- Kanamori, H., and D. L. Anderson, Theoretical basis of some empirical relations in seismology, *Bull. Seismol. Soc. Am.*, **65**, 1073–1095, 1975.

- King, J. L., and B. E. Tucker, Observed variations of earthquake motion across a sediment-filled valley, *Bull. Seismol. Soc. Am.*, *74*, 137–151, 1984.
- Kosarev, G. L., N. V. Petersen, L. P. Vinnik, and S. W. Roecker, Receiver functions for the Tien Shan analog broadband network: Contrasts in the evolution of the structures across the Talasso-Fergana fault, *J. Geophys. Res.*, *98*, 4437–4448, 1993.
- Neele, F., J. C. VanDecar, and R. Snieder, The use of P wave amplitude data in a joint inversion with travel times for upper mantle velocity structure, *J. Geophys. Res.*, *98*, 12,033–12,054, 1993.
- Nolet, G., and F. A. Dahlen, Wave front healing and the evolution of seismic delay times, *J. Geophys. Res.*, *105*, 19,043–19,054, 2000.
- Nuttli, O. W., The amplitudes of teleseismic P waves, *Bull. Seismol. Soc. Am.*, *62*, 343–356, 1972.
- Ramingwong, T., S. Ratanasathien, and S. Sertsrivanit, Geothermal resources of northern Thailand: Hydrogeologic considerations, in *Proceedings of the Third Regional conference on Geology and Mineral Resources of South-east Asia, Bangkok, Nov. 14–18*, edited by P. Nutalaya, pp. 239–251, Asian Inst. of Technol., Bangkok, Thailand, 1978.
- Tibuleac, I., G. Nolet, C. Michaelson, and I. Koulakov, P wave amplitudes in a 3D Earth, *Geophys. J. Int.*, in press, 2003.
- Vernon, F. L., G. L. Pavlis, T. J. Owens, D. E. McNamara, and P. N. Anderson, Near-surface scattering effects observed with a high-frequency phased array at Piñon Flats, California, *Bull. Seismol. Soc. Am.*, *88*, 1548–1560, 1998.

---

F. A. Dahlen, G. Nolet, and Y. Zhou, Department of Geosciences, Princeton University, Princeton, NJ 08544, USA. (fad@princeton.edu; nolet@princeton.edu; yingz@princeton.edu)



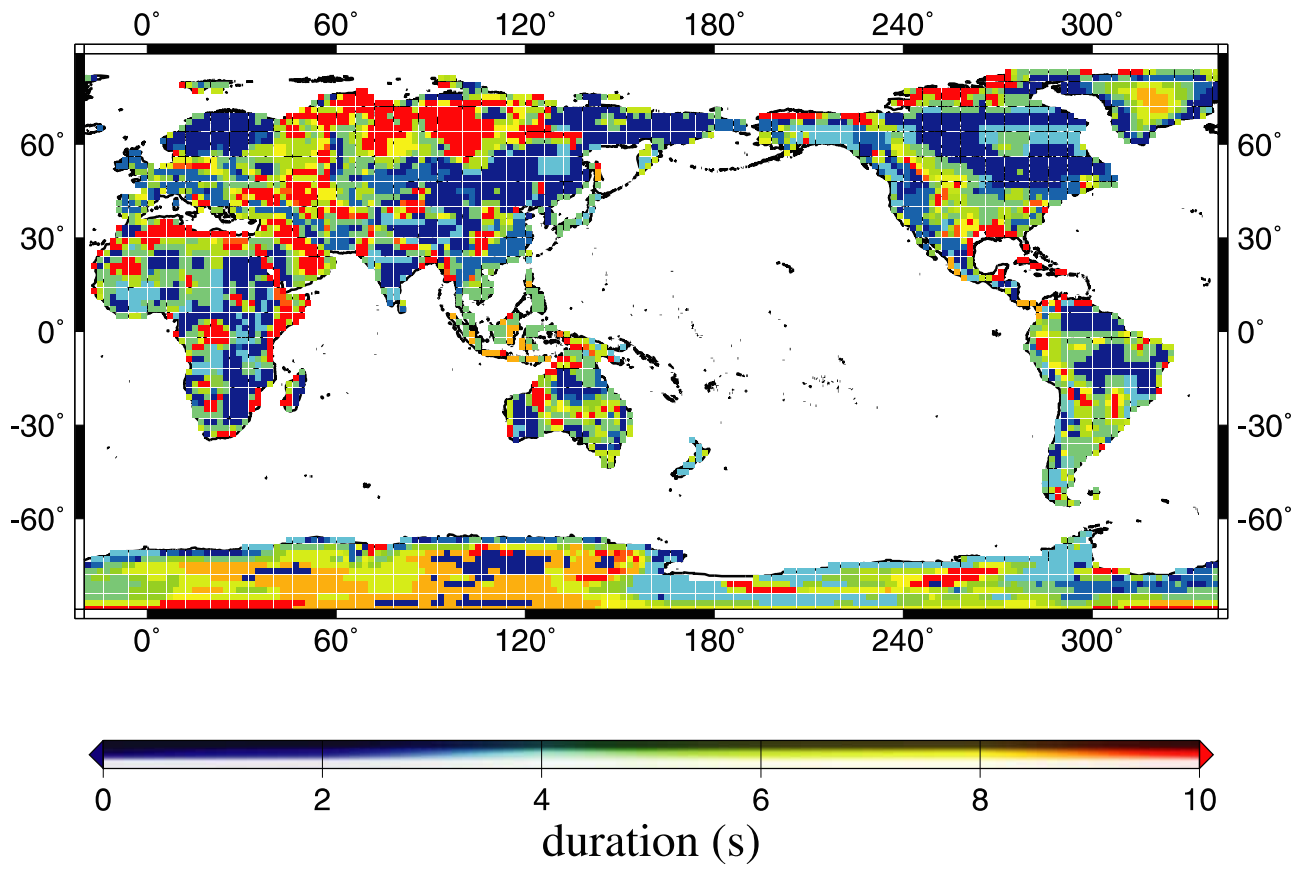


**Figure 5.** Map of the “reference” period above which the crustal amplification of teleseismic *P* wave can be regarded as frequency independent (the amplification slope  $dA/dT > -0.025$ ).